JACS
JOURNAL OF THE AMERICAN CHEMICAL SOCIETY
pubs.acs.org/JACS
Communication

A pH-Dependent Conformational Switch Controls *N. meningitidis* ClpP Protease Function

Zev A. Ripstein,*,○ Siavash Vahidi,*,○ John L. Rubinstein,* and Lewis E. Kay*

Cite This: *J. Am. Chem. Soc.* 2020, 142, 20519–20523

ABSTRACT: ClpPs are a conserved family of serine proteases that collaborate with ATP-dependent translocases to degrade protein substrates. Drugs targeting these enzymes have attracted interest for the treatment of cancer and bacterial infections due to their critical role in mitochondrial and bacterial proteostasis, respectively. As such, there is significant interest in understanding structure–function relationships in this protein family. ClpPs are known to crystallize in extended, compact, and compressed forms; however, it is unclear what conditions favor the formation of each form and whether they are populated by wild-type enzymes in solution. Here, we use cryo-EM and solution NMR spectroscopy to demonstrate that a pH-dependent conformational switch controls an equilibrium between the active extended and inactive compressed forms of ClpP from the Gram-negative pathogen *Neisseria meningitidis*. Our findings provide insight into how ClpPs exploit their rugged energy landscapes to enable key conformational changes that regulate their function.

Biomolecular machines undergo a multitude of conformational changes to perform their functions that can be understood in terms of excursions to local minima on a funneled free energy landscape.[1] These machines can exploit the ruggedness of their free energy landscapes to switch conformation in response to external stimuli. A large body of evidence suggests that the ClpP protease family exemplifies such a system. ClpP plays a critical role in maintaining proteostasis in the bacterial cytosol and in the mitochondrial matrix.[2] Therefore, there is significant interest in disrupting their tightly regulated activities to treat bacterial infections[3−5] and hematological malignancies in humans.[6−8]

The 300-kDa ClpP tetradecamer sequesters 14 His-Ser-Asp catalytic triads in a barrel-like enclosure, comprised of a pair of stacked homoheptameric rings, to limit spurious protein degradation. The main body of the barrel is formed by the head domains of the protomers. Near the equator of the barrel, the handle domains of the protomers mediate inter-ring contacts between subunits on opposite rings and play a critical role in aligning the catalytic triad (Figure 1A). Entry of substrate into the barrel is regulated via N-terminal axial pores and the binding of AAA+ motors (e.g., ClpX) that select and unfold proteins in an ATP-dependent fashion into the ClpP barrel for proteolysis.[9] One poorly understood aspect of ClpP regulation is the relationship between the structural dynamics of the complex and its function. It is well-established that the extended form of the barrel, with an intact handle domain and a fully formed catalytic triad, represents the active proteolytic conformation in solution (Figure 1A).[10] However, the extended form is unlikely to be the sole conformation populated by ClpP. For example, solution NMR studies show that the N-terminal and handle regions sample multiple conformations.[11−13] ClpP crystallizes in "compact" and "compressed" forms that mainly differ in the height of the complex and in the conformation of the handle domain.[14] The compact form exhibits a shorter barrel height and

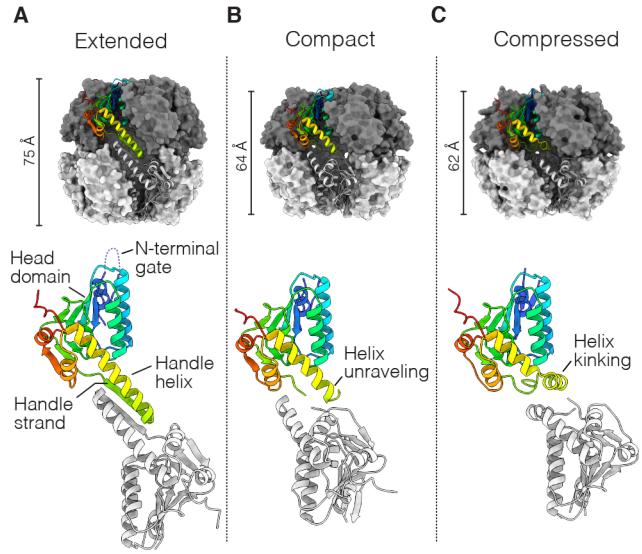

Figure 1. ClpP crystallizes in various forms. The overall architecture and a pair of opposing protomers are shown for the (A) extended (PDB 3V5E),[24] (B) compact (PDB 4EMM),[30] and (C) compressed (PDB 3QWD)[31] conformations of *Staphylococcus aureus* ClpP. In each case, the height of the ClpP barrel together with the N-terminal, head, and handle regions are highlighted. The largest structural differences occur in the handle region.

Received: September 2, 2020
Published: November 24, 2020

https://dx.doi.org/10.1021/jacs.0c09474
J. Am. Chem. Soc. 2020, 142, 20519–20523

a partially formed handle β-strand, which affects the orientation of the catalytic triad and renders it inactive (Figure 1B). The compressed form has a disordered handle β-strand and a kinked handle helix whose N-terminal portion projects into the lumen of the barrel, resulting in a misaligned catalytic triad (Figure 1C). It is unclear what conditions favor the formation of each ClpP form discussed above, whether the compressed/compact forms can be populated by wild-type enzymes outside of a crystal lattice, and if these forms are sampled in solution during ClpP function.

Changes in pH modulate the ionization states of weak acids and bases and therefore affect the structure and function of proteins. For this reason, the cellular pH affects a plethora of critical processes and is sensed and tightly controlled by a number of proton pumps and transporters.[15] For example, pH-dependent conformational switches have been shown to regulate the activity of ion[16] and water[17] channels and the function of viral[18] and bacterial[19] proteins controlling host cell entry through large-scale conformational changes. His145 on the structurally sensitive handle helix of each protomer of *Neisseria meningitidis* ClpP (NmClpP), and in a number of ClpPs from other species (Figure S1), forms a key H-bond with the catalytic Asp178 of a neighboring protomer.[20] We investigated the relationship between the protonation state of this semiconserved histidine and the solution structure of NmClpP using methyl-TROSY NMR.[21] A highly deuterated protein sample with an engineered Cys residue in the handle region (I144C) was produced (see Supporting Information) and subsequently reacted with ^{13}C-methylmethanethiosulfonate (MMTS) to generate an S-methylthio-cysteine (MTC) residue containing an NMR-visible $^{13}CH_3$-probe[12] that reports on the conformation of the handle region (Figures S2–S4; see Supporting Information discussion). Titration of ^{13}C-MTC144 NmClpP from pH 5 to 10 leads to a decrease in the intensity of the low pH peak (Figure 2A-blue) and concomitant appearance of a new resonance (Figure 2A-red), indicating slow conformational exchange on the NMR chemical shift time scale. The pH profile of the activity of ^{13}C-MTC144 NmClpP, as probed by the PKM-AMC substrate (Figure 2B-green circles; Figure S5), closely tracks the relative population of the high pH state derived from normalized peak volumes (Figure 2B-green and red). NMR titration data and the activity assays could be jointly fit to a simple Henderson–Hasselbalch model (Figure 2B-solid lines) with an apparent pK_a of 7.4 ± 0.2 that is consistent with an inactive ⇌ active interconversion triggered by the ionization of the imidazole ring of His145 adjacent to the ^{13}C-MTC144 probe (see Supporting Information).

Having established a pH dependent activity profile linked to a structural change in the handle region, we next compared three-dimensional structures of NmClpP within the ClpXP complex at pH 5 and 8.5. The structure of WT NmClpP in complex with *Neisseria meningitidis* ClpX (NmClpX) has been previously solved[22] at pH 8.5 (Figure 2C). Similar to published crystal structures of NmClpP in the active extended conformation,[20,23] the handle helix is fully formed at this pH, and the handle β-sheet is present, albeit shorter than in ClpPs from other organisms.[10,24] Key intra-ring contacts are provided via a H-bond between His145 of one protomer and the catalytic Asp178 from the adjacent protomer on the same ring (Figure 2C, inset). Consistent with the observed activity in the degradation assays (Figure 2B-green), the so-called "oligomerization sensor"[24] residues Asp176-Arg177 form a pair of inter-ring salt bridges that further help to position the catalytic Asp178 properly

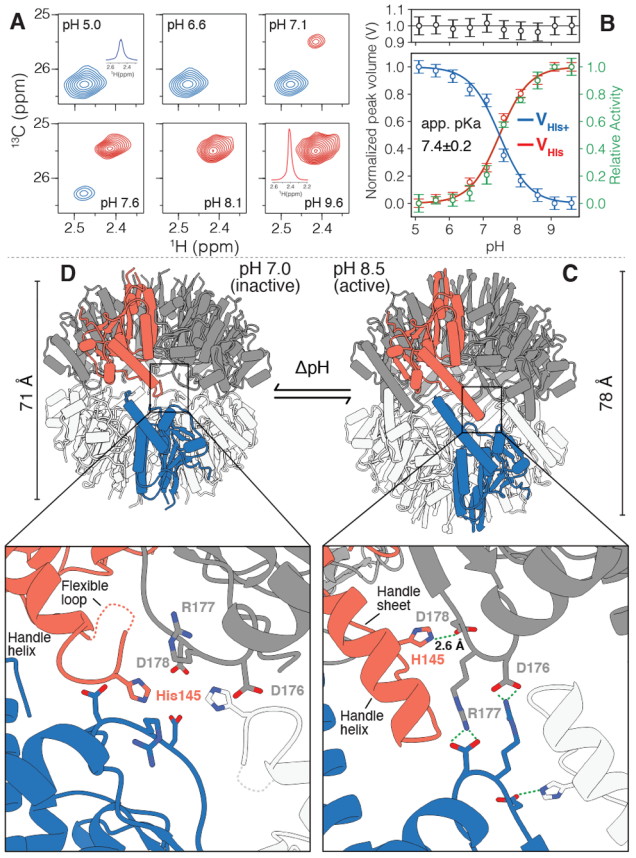

Figure 2. pH modulates the activity and structure of NmClpP. (A) ^{1}H–^{13}C HMQC spectra of [U^{2-}H]-^{13}C-MTC144 NmClpP recorded as a function of pH at 40 °C and 18.8 T indicate a slow time scale interconversion between a pair of conformers. ^{1}H traces highlight different contributions from conformational heterogeneity at extreme pH values. (B) Changes in the normalized peak volumes (V_{His+} = V_{His+}(pH)/V_{His+}(pH 5.0) and V_{His} = V_{His}(pH)/V_{His}(pH 9.6)) of the blue and red peaks in A as a function of pH. Error bars are derived from noise levels in each spectrum. (top, black) V_{His+} and V_{His} report fractional populations of each of the two states with V_{His+} + V_{His} = 1. (bottom) Activity of [U–^{2}H]-^{13}C-MTC144 NmClpP measured as a function of pH using 250 μM PKM-AMC as substrate in $^{2}H_2O$-based buffer, 40 °C (green circles; see Supporting Information). Solid lines are global fits of relative populations based on normalized peak volumes in NMR spectra and activity measurements to a simple Henderson–Hasselbalch ionization model (see Supporting Information). Cryo-EM structures of WT NmClpP in complex with NmClpX (not shown) at (C) pH 8.5 (PDBID 6VFS[22]) and (D) pH 7.0. In each case, a pair of opposing protomers are colored red and blue to highlight the ring–ring interaction interface. The height of the ClpP barrel (excluding the N termini) is denoted, and the statuses of the oligomerization sensor in wild-type NmClpP at pH 8.5 and 7.0 are indicated in the insets. Major structural differences in the handle region are highlighted. Side chains of residues involved in the formation of inter-ring salt-bridges and intra-ring H-bonds are indicated. Similar structural features as described above were observed for isolated NmClpP at pH 7.0 and 8.5 (Figure S9).

(Figure 2C, inset). To obtain the structure of the inactive form, a solution containing NmClpXP was adjusted to pH 7.0, and vitrified samples for cryo-EM analysis were prepared as described previously.[22] The resulting 3.1 Å resolution structure of doubly capped NmClpXP (Figures S6–S11) reveals that the ClpP barrel is in a compressed conformation, characterized by a shorter barrel height of 71 Å (Figure 2D) versus a height of 78 Å

https://dx.doi.org/10.1021/jacs.0c09474
J. Am. Chem. Soc. 2020, 142, 20519–20523

measured for the extended form (Figure 2C). Notably, the handle helix is broken near His145 and shortened by seven residues or roughly two turns with residues 138−145 no longer helical and now pointing toward the interior of the ClpP barrel (Figure 2D). Disorder and flexibility in the handle region are also evident from the local resolution map that shows lower resolution in the handle region compared to the well-structured head domain (Figure S8). The His145-Asp178 intra-ring H-bond and the inter-ring oligomerization sensor salt bridges are lost, resulting in misalignment of the catalytic triad. Protonated histidine residues have low helical propensity, especially when positioned near the N terminus of a helix, because of interactions with the helix dipole.[25,26] Therefore, the pH-dependent partial unraveling of the handle helix and loss of activity is likely caused by the protonation of the His145 side chain.

Our work shows that the handle region governs an inactive ⇌ active equilibrium in NmClpP in response to pH changes with an apparent pK_a of 7.4 ± 0.2. At physiological pH, both the extended and compressed states of NmClpP coexist in solution, while a small pH change leads to large modulations of ClpP activity (Figure 2B, 3A). The plasticity of the handle region plays

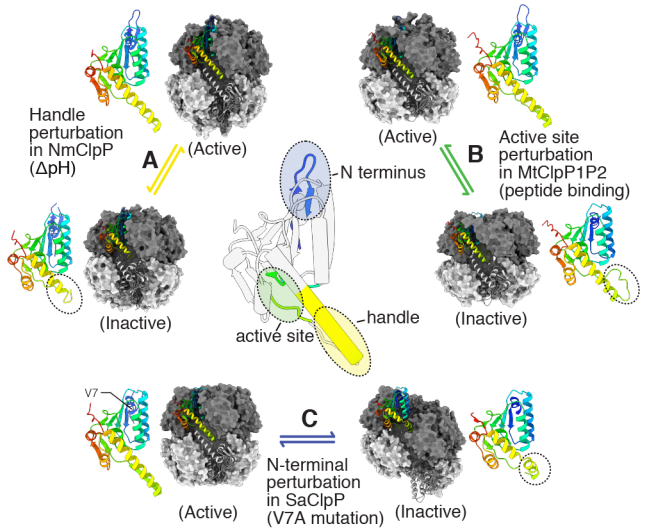

Figure 3. ClpPs have rugged energy landscapes. (A−C) Conformational equilibria of ClpP from different species. (A) A pH-sensitive handle region leads to a pair of conformations for NmClpP at physiological pH in which part of the handle helix is unraveled in the inactive state. (B) Binding of short peptide substrate-mimics to the active sites of MtClpP1P2 shifts the equilibrium from the inactive compact form (PDB 6VGK)[27] to the active extended state (PDB 5DZK).[32] (C) Perturbation of the N-terminal region via a V7A mutation affects the global structure of SaClpP, including the handle region (PDBs 6DKF and 3V5E).[13,24]

an integral role in the function of *Mycobacterium tuberculosis* ClpP1P2 (MtClpP1P2), where the compact:extended equilibrium is heavily skewed toward the inactive compact state to prevent spurious protein degradation.[27] In this case, the active extended form becomes populated via a highly cooperative transition in which substrate-like dipeptides bind substoichiometrically at the active sites (Figure 3B). A similar transition from the compact to the extended form had been shown to be triggered by the binding of active site inhibitors in *Thermus thermophilus* ClpP.[28] Regulation of proteolysis via conformational control of ClpPs can also occur by perturbations to the gate region. This phenomenon is highlighted by the V7A mutant of *Staphylococcus aureus* ClpP (SaClpP), which forms a noncanonical lock-washer architecture comprised of protomers with different structural features, some of which contain shortened and kinked handle helices[13] (Figure 3C). The active extended form of the enzyme can be restored via the binding of ADEP activators,[13] further demonstrating the plasticity of ClpP.

Intriguingly, recent structures of the AAA+ Lon protease[29] provide strong evidence that conformational switching is important in regulating other proteases. Lon is predominantly in an inactive conformation (LonOFF)[29] that resembles the lock-washer structure of V7A SaClpP. In LonOFF, both the unfoldase and the protease components are in a left-handed spiral, with the substrate binding groove of the protease occluded and the Lys-Ser catalytic dyad distorted. Analogous to activation of V7A SaClpP by ADEP,[13] LonOFF undergoes an allosteric reorganization upon addition of ATP and substrate to assemble the enzymatically active C6-symmetric hexamer. It is likely that the inherent conformational plasticity of molecular machines, such as ClpP and Lon, can be exploited to discover novel avenues to manipulate their function. Detailed structure−function investigations, such as the combined NMR and cryo-EM approach applied here, are uniquely suited to provide insight into how this might be accomplished.

■ ASSOCIATED CONTENT

Supporting Information

The Supporting Information is available free of charge at https://pubs.acs.org/doi/10.1021/jacs.0c09474.

Supporting Figures 1−11, including sequence alignments, NMR and cryo-EM data, description of protein production and labeling, activity assays, and data collection and analysis (PDF)

■ AUTHOR INFORMATION

Corresponding Authors

Zev A. Ripstein − *Department of Biochemistry, University of Toronto, Toronto, Ontario M5S 1A8, Canada; Program in Molecular Medicine, Hospital for Sick Children, Toronto, Ontario M5G 1X8, Canada;* orcid.org/0000-0003-3601-0596; Email: zevripstein@gmail.com

Siavash Vahidi − *Department of Biochemistry, Department of Molecular Genetics, and Department of Chemistry, University of Toronto, Toronto, Ontario M5S 1A8, Canada; Program in Molecular Medicine, Hospital for Sick Children, Toronto, Ontario M5G 1X8, Canada;* orcid.org/0000-0001-8637-3710; Email: svahidi@uoguelph.ca

Lewis E. Kay − *Department of Biochemistry, Department of Molecular Genetics, and Department of Chemistry, University of Toronto, Toronto, Ontario M5S 1A8, Canada; Program in Molecular Medicine, Hospital for Sick Children, Toronto, Ontario M5G 1X8, Canada;* orcid.org/0000-0002-4054-4083; Email: kay@pound.med.utoronto.ca

John L. Rubinstein − *Department of Biochemistry and Department of Medical Biophysics, University of Toronto, Toronto, Ontario M5S 1A8, Canada; Program in Molecular Medicine, Hospital for Sick Children, Toronto, Ontario M5G 1X8, Canada*; Email: john.rubinstein@utoronto.ca

Complete contact information is available at: https://pubs.acs.org/10.1021/jacs.0c09474

Author Contributions

○Z.A.R. and S.V. contributed equally.

https://dx.doi.org/10.1021/jacs.0c09474
J. Am. Chem. Soc. 2020, 142, 20519−20523

Notes

The authors declare no competing financial interest.

■ ACKNOWLEDGMENTS

We thank Dr. Samir Benlekbir for assistance with cryo-EM data collection. Z.A.R. and S.V. were supported by a scholarship and a postdoctoral fellowship, respectively, from the Canadian Institutes of Health Research (CIHR). This research was funded by CIHR grants MOP-133408 (L.E.K.) and PJT-162186 (J.L.R.) and supported by the Canada Research Chairs program. Titan Krios cryo-EM data were collected at the Toronto High-Resolution High-Throughput cryo-EM facility supported by the Canadian Foundation for Innovation and Ontario Research Fund.

■ REFERENCES

(1) Karplus, M.; Kuriyan, J. Molecular Dynamics and Protein Function. *Proc. Natl. Acad. Sci. U. S. A.* **2005**, *102* (19), 6679−6685.
(2) Bhandari, V.; Wong, K. S.; Zhou, J. L.; Mabanglo, M. F.; Batey, R. A.; Houry, W. A. The Role of ClpP Protease in Bacterial Pathogenesis and Human Diseases. *ACS Chem. Biol.* **2018**, *13* (6), 1413−1425.
(3) Brotz-Oesterhelt, H.; Beyer, D.; Kroll, H.-P.; Endermann, R.; Ladel, C.; Schroeder, W.; Hinzen, B.; Raddatz, S.; Paulsen, H.; Henninger, K.; Bandow, J. E; Sahl, H.-G.; Labischinski, H. Dysregulation of Bacterial Proteolytic Machinery by a New Class of Antibiotics. *Nat. Med.* **2005**, *11*, 1082−1087.
(4) Culp, E.; Wright, G. D. Bacterial Proteases, Untapped Antimicrobial Drug Targets. *J. Antibiot.* **2017**, *70* (4), 366−377.
(5) Gerdes, K.; Ingmer, H. Killing the Survivors. *Nature* **2013**, *503*, 347−349.
(6) Wong, K. S.; Mabanglo, M. F.; Seraphim, T. V.; Mollica, A.; Mao, Y.-Q.; Rizzolo, K.; Leung, E.; Moutaoufik, M. T.; Hoell, L.; Phanse, S.; Goodreid, J.; Barbosa, L. R. S.; Ramos, C. H. I.; Babu, M.; Mennella, V.; Batey, R. A.; Schimmer, A. D.; Houry, W. A. Acyldepsipeptide Analogs Dysregulate Human Mitochondrial ClpP Protease Activity and Cause Apoptotic Cell Death. *Cell Chem. Biol.* **2018**, *25* (8), 1017−1030.
(7) Ishizawa, J.; Zarabi, S. F.; Davis, R. E.; Halgas, O.; Nii, T.; Jitkova, Y.; Zhao, R.; St-Germain, J.; Heese, L. E.; Egan, G.; Ruvolo, V. R.; Barghout, S. H.; Nishida, Y.; Hurren, R.; Ma, W.; Gronda, M.; Link, T.; Wong, K.; Mabanglo, M.; Kojima, K.; Borthakur, G.; MacLean, N.; Ma, M. C. J.; Leber, A. B.; Minden, M. D.; Houry, W.; Kantarjian, H.; Stogniew, M.; Raught, B.; Pai, E. F.; Schimmer, A. D.; Andreeff, M. Mitochondrial ClpP-Mediated Proteolysis Induces Selective Cancer Cell Lethality. *Cancer Cell* **2019**, *35* (5), 721−737.
(8) Stahl, M.; Korotkov, V.; Balogh, D.; Kick, L.; Gersch, M.; Pahl, A.; Kielkowski, P.; Richter, K.; Schneider, S.; Sieber, S. A. Selective Activation of Human Caseinolytic Protease P (ClpP). *Angew. Chem., Int. Ed.* **2018**, *57* (44), 14602−14607.
(9) Kress, W.; Maglica, Z.; Weber-Ban, E. Clp Chaperone-Proteases: Structure and Function. *Res. Microbiol.* **2009**, *160* (9), 618−628.
(10) Wang, J.; Hartling, J. A.; Flanagan, J. M. The Structure of ClpP at 2.3 A° Resolution Suggests a Model for ATP-Dependent Proteolysis. *Cell* **1997**, *91*, 447−456.
(11) Sprangers, R.; Gribun, A.; Hwang, P. M.; Houry, W. A.; Kay, L. E. Quantitative NMR Spectroscopy of Supramolecular Complexes: Dynamic Side Pores in ClpP Are Important for Product Release. *Proc. Natl. Acad. Sci. U. S. A.* **2005**, *102*, 16678−16683.
(12) Religa, T. L.; Ruschak, A. M.; Rosenzweig, R.; Kay, L. E. Site-Directed Methyl Group Labeling as an NMR Probe of Structure and Dynamics in Supramolecular Protein Systems: Applications to the Proteasome and to the ClpP Protease. *J. Am. Chem. Soc.* **2011**, *133* (23), 9063−9068.
(13) Vahidi, S.; Ripstein, Z. A.; Bonomi, M.; Yuwen, T.; Mabanglo, M. F.; Juravsky, J. B.; Rizzolo, K.; Velyvis, A.; Houry, W. A.; Vendruscolo, M.; Rubinstein, J. L.; Kay, L. E. Reversible Inhibition of the ClpP Protease via an N-Terminal Conformational Switch. *Proc. Natl. Acad. Sci. U. S. A.* **2018**, *115* (28), E6447−E6456.
(14) Liu, K.; Ologbenla, A.; Houry, W. A. Dynamics of the ClpP Serine Protease: A Model for Self-Compartmentalized Proteases. *Crit. Rev. Biochem. Mol. Biol.* **2014**, *49* (5), 400−412.
(15) Boron, W. F. Regulation of Intracellular PH. *Adv. Physiol. Educ.* **2004**, *28* (4), 160−179.
(16) Swartz, K. J. Towards a Structural View of Gating in Potassium Channels. *Nat. Rev. Neurosci.* **2004**, *5* (12), 905−916.
(17) Törnroth-Horsefield, S.; Wang, Y.; Hedfalk, K.; Johanson, U.; Karlsson, M.; Tajkhorshid, E.; Neutze, R.; Kjellbom, P. Structural Mechanism of Plant Aquaporin Gating. *Nature* **2006**, *439* (7077), 688−694.
(18) Kass, I.; Arkin, I. T. How PH Opens a H+ Channel: The Gating Mechanism of Influenza A M2. *Structure* **2005**, *13* (12), 1789−1798.
(19) Schuerch, D. W.; Wilson-Kubalek, E. M.; Tweten, R. K. Molecular Basis of Listeriolysin O PH Dependence. *Proc. Natl. Acad. Sci. U. S. A.* **2005**, *102* (35), 12537−12542.
(20) Mabanglo, M. F.; Leung, E.; Vahidi, S.; Seraphim, T. V.; Eger, B. T.; Bryson, S.; Bhandari, V.; Zhou, J. L.; Mao, Y.-Q.; Rizzolo, K.; Barghash, M. M.; Goodreid, J. D.; Phanse, S.; Babu, M.; Barbosa, L. R. S.; Ramos, C. H. I.; Batey, R. A.; Kay, L. E.; Pai, E. F.; Houry, W. A. ClpP Protease Activation Results from the Reorganization of the Electrostatic Interaction Networks at the Entrance Pores. *Commun. Biol.* **2019**, *2* (1), 410.
(21) Tugarinov, V.; Hwang, P. M.; Ollerenshaw, J. E.; Kay, L. E. Cross-Correlated Relaxation Enhanced 1H−13C NMR Spectroscopy of Methyl Groups in Very High Molecular Weight Proteins and Protein Complexes. *J. Am. Chem. Soc.* **2003**, *125* (34), 10420−10428.
(22) Ripstein, Z. A.; Vahidi, S.; Houry, W. A.; Rubinstein, J. L.; Kay, L. E. A Processive Rotary Mechanism Couples Substrate Unfolding and Proteolysis in the ClpXP Degradation Machinery. *eLife* **2020**, *9*, No. e52158.
(23) Goodreid, J. D.; Janetzko, J.; Santa Maria, J. P.; Wong, K. S.; Leung, E.; Eger, B. T.; Bryson, S.; Pai, E. F.; Gray-Owen, S. D.; Walker, S.; Houry, W. A.; Batey, R. A. Development and Characterization of Potent Cyclic Acyldepsipeptide Analogues with Increased Antimicrobial Activity. *J. Med. Chem.* **2016**, *59* (2), 624−646.
(24) Gersch, M.; List, A.; Groll, M.; Sieber, S. A. Insights into Structural Network Responsible for Oligomerization and Activity of Bacterial Virulence Regulator Caseinolytic Protease P (ClpP) Protein. *J. Biol. Chem.* **2012**, *287* (12), 9484−9494.
(25) Armstrong, K. M.; Baldwin, R. L. Charged Histidine Affects Alpha-Helix Stability at All Positions in the Helix by Interacting with the Backbone Charges. *Proc. Natl. Acad. Sci. U. S. A.* **1993**, *90* (23), 11337−11340.
(26) Chakrabartty, A.; Kortemme, T.; Baldwin, R. L. Helix Propensities of the Amino Acids Measured in Alanine-Based Peptides without Helix-Stabilizing Side-Chain Interactions. *Protein Sci.* **1994**, *3* (5), 843−852.
(27) Vahidi, S.; Ripstein, Z. A.; Juravsky, J. B.; Rennella, E.; Goldberg, A. L.; Mittermaier, A. K.; Rubinstein, J. L.; Kay, L. E. An Allosteric Switch Regulates Mycobacterium Tuberculosis ClpP1P2 Protease Function as Established by Cryo-EM and Methyl-TROSY NMR. *Proc. Natl. Acad. Sci. U. S. A.* **2020**, *117* (11), 5895−5906.
(28) Felix, J.; Weinhäupl, K.; Chipot, C.; Dehez, F.; Hessel, A.; Gauto, D. F.; Morlot, C.; Abian, O.; Gutsche, I.; Velazquez-Campoy, A.; Schanda, P.; Fraga, H. Mechanism of the Allosteric Activation of the ClpP Protease Machinery by Substrates and Active-Site Inhibitors. *Sci. Adv.* **2019**, *5* (9), No. eaaw3818.
(29) Shin, M.; Puchades, C.; Asmita, A.; Puri, N.; Adjei, E.; Wiseman, R. L.; Karzai, A. W.; Lander, G. C. Structural Basis for Distinct Operational Modes and Protease Activation in AAA+ Protease Lon. *Sci. Adv.* **2020**, *6* (21), No. eaba8404.
(30) Ye, F.; Zhang, J.; Liu, H. C.; Hilgenfeld, R.; Zhang, R. H.; Kong, X. Q.; Li, L. C.; Lu, J. Y.; Zhang, X. L.; Li, D. H.; Jiang, H. L.; Yang, C. G.; Luo, C. Helix Unfolding/Refolding Characterizes the Functional Dynamics of Staphylococcus Aureus Clp Protease. *J. Biol. Chem.* **2013**, *288* (24), 17643−17653.

https://dx.doi.org/10.1021/jacs.0c09474
J. Am. Chem. Soc. 2020, 142, 20519−20523

(31) Geiger, S. R.; Bottcher, T.; Sieber, S. A.; Cramer, P. A Conformational Switch Underlies ClpP Protease Function. *Angew. Chem., Int. Ed.* **2011**, *50*, 5749−5752.
(32) Li, M.; Kandror, O.; Akopian, T.; Dharkar, P.; Wlodawer, A.; Maurizi, M. R.; Goldberg, A. L. Structure and Functional Properties of the Active Form of the Proteolytic Complex, ClpP1P2, from Mycobacterium Tuberculosis. *J. Biol. Chem.* **2016**, *291* (14), 7465−7476.

https://dx.doi.org/10.1021/jacs.0c09474
J. Am. Chem. Soc. 2020, 142, 20519−20523